

# Super-regenerative Receiver for UWB-FM

Rui Hou, Nitz Saputra and John R. Long

Electronic Research Laboratory, Faculty of EEMCS, Delft University of Technology

Mekelweg 4, Room 18.280, 2628 CD Delft, the Netherlands

Phone: +31 (0)15 2782006, Email: r.hou@student.tudelft.nl

**Abstract**—UWB-FM is a low-complexity ultra-wideband (UWB) communication system designed for short-range, low-data-rate wireless applications. A fully integrated super-regenerative receiver in IBM 90-nm RF CMOS technology is designed to detect 500 MHz bandwidth UWB-FM signals at 4.5 GHz. Circuit simulations show that a receiver sensitivity of  $-82.2$  dB is attainable for a 100 kbps baseband data-rate and  $10^{-6}$  potential bit-error-rate. The whole receiver draws an average of 2 mA from a 0.9 V supply.

**Index Terms**—low-power, super-regenerative receiver, UWB-FM

## I. INTRODUCTION

The recent advance of short-range communication technologies such as personal area networks (PAN) and wireless sensor networks (WSN) create immense application possibilities, ranging from clinical diagnosis to wildlife monitoring. These applications require simple receivers with low power-consumption, since consumer products with bulky batteries are unattractive and field deployment of ephemeral sensors is unacceptable.

UWB-FM [1] is a low-power low-complexity ultra-wideband (UWB) modulation scheme designed for short-range, low-data-rate PAN and WSN applications. It utilizes the wideband frequency modulation (WBFM) to spread the spectrum of a continuous carrier over a large bandwidth. Compared with narrow-band modulation schemes such as on-off keying (OOK), UWB-FM offers low-cost wireless links since the spectrum licensing fee is avoided. Furthermore, the continuous carrier mitigates the necessity of synchronization, so that the complexity and power consumption of receivers are reduced. Previous work utilizes delay-line demodulators for UWB-FM detection. The reported power consumption is between 10 to 20 mW [2], [3].

The goal of this research is to further reduce the power consumption of a UWB-FM receiver by exploiting the super-regeneration principle [4]. Employing positive feedback, super-regenerative receivers operate in an intermittent oscillatory condition. Oscillations are periodically built up from weak RF excitations and then quenched to avoid amplification saturation. In doing so, a huge amount of gain can be obtained by a single stage.

Typically, super-regenerative receivers have been designed for simple narrow-band modulation schemes such as OOK [5]–[10], providing that proper measures [11] are taken to improve the poor selectivity and inherent frequency instability. Occasionally, they were also used to detect spread spectrum [12], [13] and pulse based UWB signals [14]–[16], benefiting from

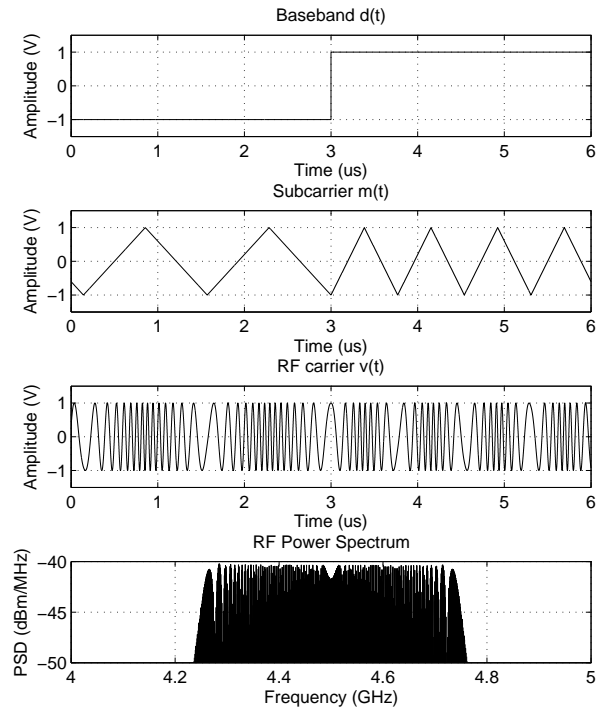


Figure 1. The time-domain waveforms of the baseband data, subcarrier, RF UWB-FM signal and its spectrum.

the alleviated selectivity and frequency-stability requirements of these applications.

The classical way of applying super-regeneration principle to FM detection is based on the slope demodulation process [17]. In essence, a super-regenerator is detuned from the RF center frequency so as to generate a variable gain for frequency variations. Other techniques [18], [19] are also seen in the literature.

## II. RECEIVER ARCHITECTURE

### A. UWB-FM Reception

UWB-FM involves double frequency modulations (FM), a low modulation-index frequency shift keying (FSK) followed by a high modulation-index analog FM. The double FM scheme is illustrated in Fig. 1. As shown in the graph, a digital baseband signal,  $d(t)$ , having a data rate of 20, 40 or 100 kbps, modulates a triangular subcarrier of 1-2 MHz,  $m(t)$ , using FSK with a modulation index of 1. The subcarrier,

Table I  
RECEIVER SPECIFICATIONS.

Parameter	Value
RF center frequency	4.5 GHz
RF bandwidth	500 MHz
Subcarrier frequency	1 MHz
Subcarrier modulation	FSK, $\beta = 1$
Baseband data-rate	100 kbps
Bit error rate	$10^{-6}$
Sensitivity	-80 dBm
Noise figure	-4 dB
Spurious emission	-47 dBm

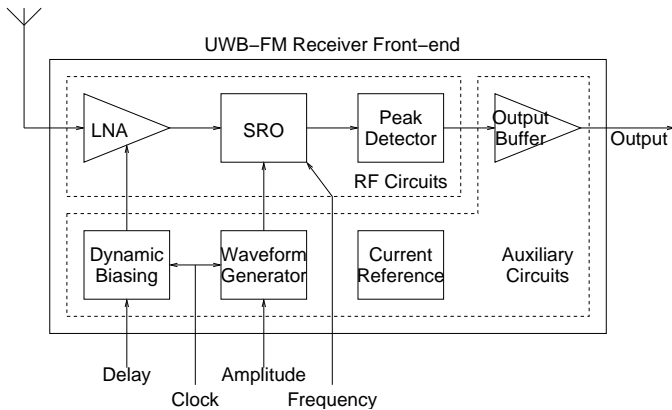


Figure 2. Block diagram of the super-regenerative receiver for UWB-FM.

$m(t)$ , then modulates the RF carrier of 3-5 GHz,  $v(t)$ , using FM, to spread its spectrum to a bandwidth of 500 MHz. The modulation indexes and the RF carrier frequency shown in the graph have been modified for the sake of visibility. The power spectrum of a UWB-FM signal centered at 4.5 GHz, being modulated by a 1 MHz triangular wave, is shown at the bottom of the figure. The low-cost low-power demodulation of this signal to reconstruct the subcarrier is the objective of this receiver.

The specifications of the receiver are derived from the application background, summarized in Table I.

### B. Receiver Structure

The block diagram of the super-regenerative receiver is shown in Fig. 2. The LNA feeds the RF signal received from the antenna into the super-regenerative oscillator (SRO). It suppresses the noise of following stages, shifts up the antenna impedance in order not to load the SRO and shields the high-power oscillation from coupling back into the antenna. The SRO, being the key component of this receiver, provides the major amplification and converts the incoming signal from FM into amplitude modulation (AM). The oscillation envelope is then extracted by the peak detector and output via a voltage buffer.

The optimum FM-AM conversion of the SRO requires a certain quenching waveform which is produced by the waveform generator. During the quenching period, LNA is turned off by the dynamic biasing circuit in order to save power.

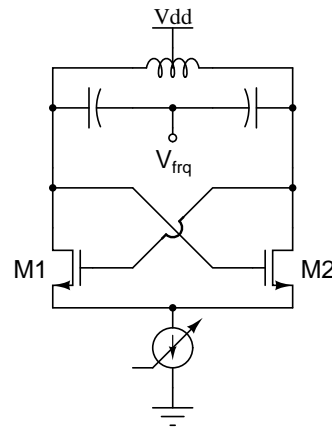


Figure 3. The schematic of the super-regenerative oscillator.

## III. CIRCUIT IMPLEMENTATION

### A. Super-regenerative Oscillator

The schematic of the super-regenerative oscillator is plotted in Fig. 3. Its topology is identical with a classical NMOS negative-GM oscillator. An on-chip LC resonator is used as the frequency selective network. The cross-coupled pair of transistors M1 and M2 generates a negative conductance to compensate the loss of the LC tank. A time-varying biasing current yields the periodical build-up of oscillations.

When the incoming signal is at the oscillator's center frequency, 4.5 GHz, the initiated oscillation has the maximum amplitude, as shown in Fig. 4. When the excitation signal deviates from the center frequency, oscillations still grow up, but their amplitudes are reduced. At the maximum frequency deviation of 4.25 or 4.75 GHz, oscillations triggered by the RF signal have the minimum amplitudes. In this way, an FM signal is converted into AM oscillation pulses. A saw-tooth like quenching current waveform, shown at the bottom of the figure is required for the optimum FM-AM conversion.

### B. Quenching Waveform Generator

The current waveform shown in Fig. 4, which consists of a gradual current increase followed by a sharp quench, is produced by the quenching waveform generator. Since the direct generation of the current ramp needs an inductor to integrate voltage, which leads to a large chip area, this design applies an indirect method. First, a voltage ramp is produced by a capacitor integrating a current. Then, it is converted into current by a linear transconductor.

The schematic of this quenching waveform generator is shown in Fig. 5. At the left half of the circuit, an external DC voltage  $V_{amp}$  is converted to a DC current by  $R_i$ . The current is then mirrored to the switched-capacitor circuit. When switch M1 is open and M2 is closed, the current gradually charges the capacitor. After a clock transition, M2 becomes open and M1 is closed, which discharge the capacitor abruptly. In this way, the quenching waveform is produced in the voltage form, shown in the middle of Fig. 6.

The linear transconductor shown at the right of Fig. 6 converts the voltage waveform into a current. For a given gate

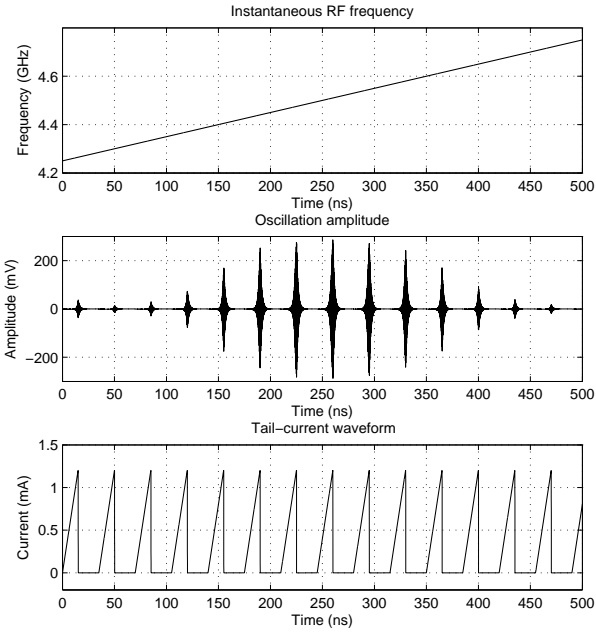


Figure 4. The excitation frequency, output oscillations and the quenching current waveform.

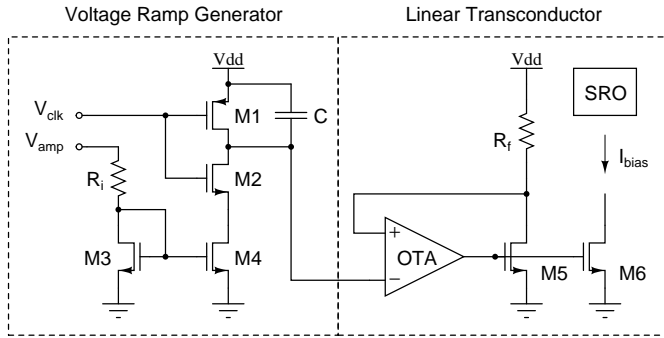


Figure 5. The schematic of the quenching waveform generator.

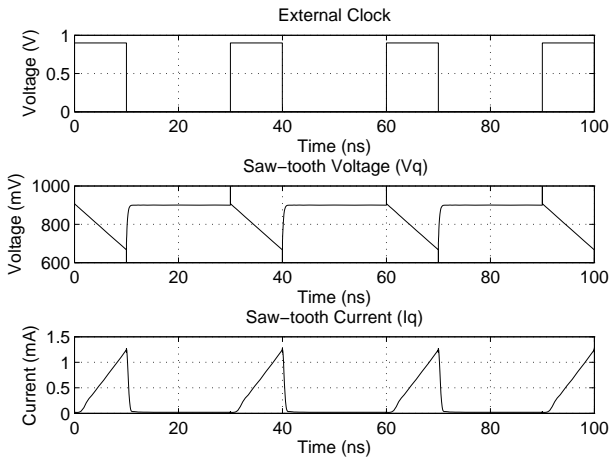


Figure 6. Quenching voltage and current waveforms.

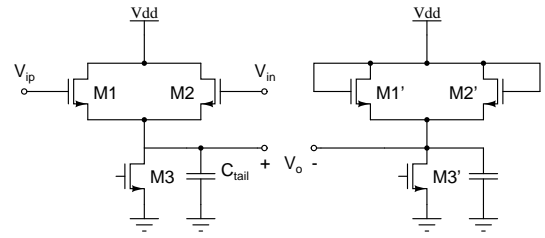


Figure 7. The differential NMOS peak detector.

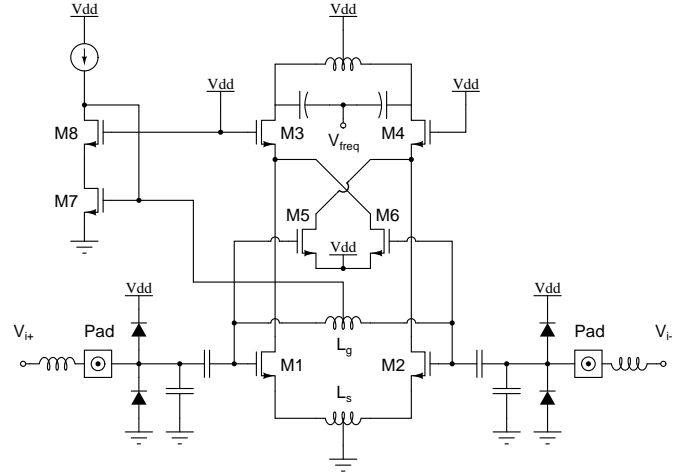


Figure 8. The schematic of the LNA.

voltage of M5, a current is generated at its drain. Resistor  $R_f$  feeds the current back as a voltage to the positive input of the operational transconductance amplifier (OTA), which compares the feedback voltage with the reference waveform and generates an error voltage to control the gate of M5.

### C. Peak Detector

The peak detector extracts the envelope of oscillations output by the SRO. Its schematic is shown in Fig. 7. Transistors M1 and M2 are biased in deep sub-inversion to perform as diodes. When the input voltage  $V_{ip}$  ( $V_{in}$ ) is larger than the source voltage  $V_{o+}$ , transistor M1 (M2) is conducting and the voltage across capacitor  $C_{tail}$  tracks the growth of the input. After a peak of a sinusoidal wave, the instantaneous input voltage  $V_{ip}$  ( $V_{in}$ ) begins to drop, transistor M1 (M2) is turned off and  $C_{tail}$  holds the peak voltage. The current source M3 slowly discharges  $C_{tail}$  in such a way that when the next peak comes,  $V_{o+}$  is again smaller than  $V_{ip}$  ( $V_{in}$ ), so every peak of a sinusoidal wave can be tracked and held, and the envelope of the fast-varying sinusoidal wave is extracted. A duplicated circuit, consisting of M1'-M3' are used to cancel the DC biasing voltage of the output envelope.

### D. LNA

The LNA is an inductively-degenerated differential common-source stage with cascode and neutralization, as shown in Fig. 8. The input resistance of the LNA is matched to 100 ohm differential antenna for maximum power transmission. The output resistance is cascoded to a large value so as

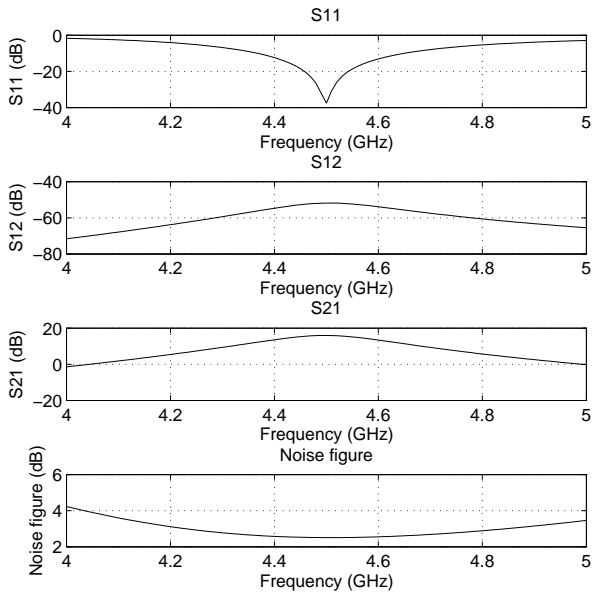


Figure 9. LNA performance.

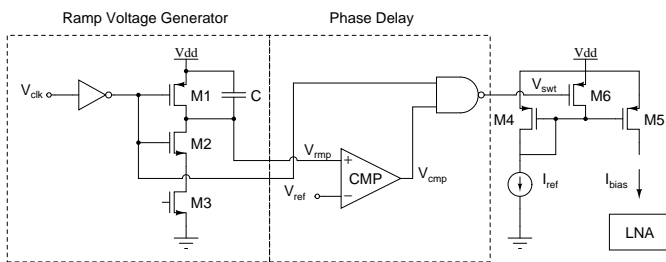


Figure 10. The schematic of the dynamic biasing network for LNA.

not to load the LC tank of the oscillator. Reverse isolation is provided by both the cascode transistors M3 and M4, and the neutralization capacitors M5 and M6. The parasitics of bondwires, bondpads and electrostatic discharge (ESD) devices are considered for the impedance matching.

The performance of the LNA is shown in Fig. 9. We observe that the input matching network has a bandwidth of 860 MHz, the reverse isolation is at least 52 dB. The forward power gain is 16 dB and the noise figure is below 3 dB in the band of interest.

### E. Dynamic LNA Biasing

The receiver does not need LNA to work when the SRO is quenched, so turning it off at the quenching period saves power. The LNA biasing cannot be controlled by the same clock used to quench the SRO. Since the LNA has a slower starting than the oscillations, it should be turned on before the start-up of the SRO. This function is provided by the dynamic LNA biasing circuit shown in Fig. 10.

The voltage-ramp generator, similar to the one shown in Fig. 5 converts the negative portion of the clock into a voltage ramp, as shown in the second row of Fig. 11. A comparator

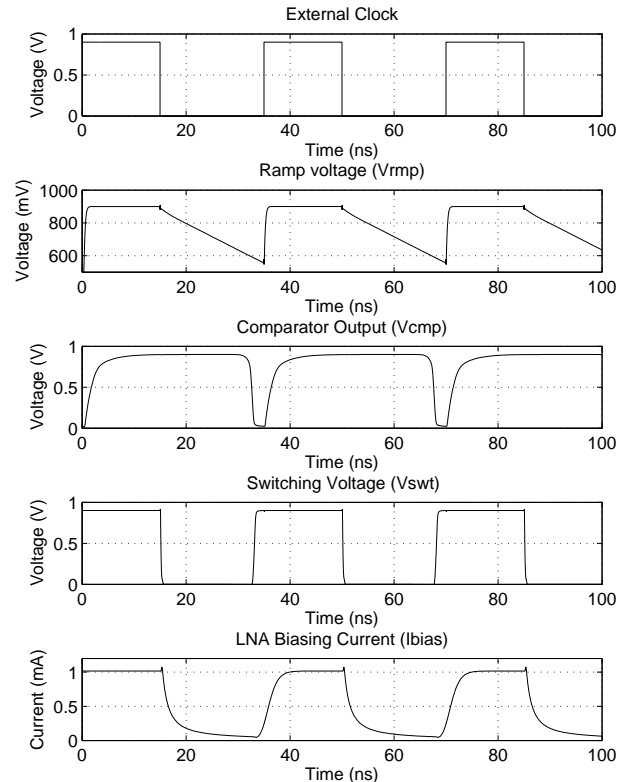


Figure 11. Dynamic LNA biasing waveforms.

compares the ramping voltage to a DC reference so the negative clock-transition is not immediately followed until the ramping voltage reaches the reference value. A warm-up period is produced for the LNA, as shown in the third row of Fig. 11. A NAND gate guarantees that the LNA works at both the warm-up period and the working period of the SRO. The quenching voltage, shown in the fourth row of Fig. 11, controls a switch which pulls up the gate voltage of the biasing current-mirror in the quenching period. The resulting dynamic biasing current for the LNA is shown at the bottom of Fig. 11.

## IV. RECEIVER PERFORMANCE

All the circuit blocks presented in the previous section are connected together and a transistor-level simulation is performed to examine the overall performance. At the input side of the receiver, a UWB-FM signal with -80 dBm RF power is applied as the excitation. An ideal second-order Butterworth bandpass filter with a center frequency of 2 MHz and a bandwidth of 400 kHz is connected to the output of the receiver.

A transient simulation is performed and its result is plotted in Fig. 12. As shown in the graph, the receiver is capable of recovering the subcarrier. Since the FM signal is converted to a 100% modulated AM signal, and the noncoherent detection of this double-sideband AM signal neglects the phase information

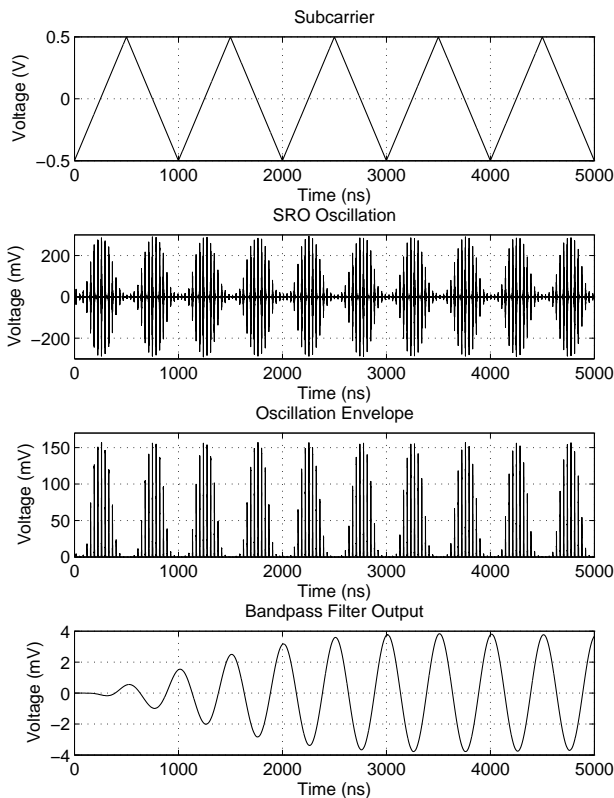


Figure 12. Simulated signals at the receiver: sub-carrier input (top), SRO output (2nd), envelope output (3rd) and bandpass filter output (bottom).

Table II  
PERFORMANCE COMPARISON OF UWB-FM RECEIVERS.

	Tong [3]	Gerrits [2]	This work
RF frequency	4 GHz	4 GHz	4.5 GHz
RF bandwidth	2 GHz	500 MHz	500 MHz
Sensitivity	N/A	-74 dBm	-83.3 dBm
Data rate	N/A	62.5 kbps	100 kbps
Bit error rate	N/A	$10^{-4}$	$10^{-6}$
Power	19.4 mW	9.6 mW (w/o LNA)	2.0 mW
Technology	0.18 $\mu$ m CMOS	0.18 $\mu$ m BiCMOS	90 nm CMOS

completely, the 1 MHz subcarrier is recovered as a 2 MHz signal.

Transient noise simulations are performed to evaluate the receiver response to noise. The output signal-to-noise ratio (SNR) of 14.3 dB is calculated by the root-mean-square value of the signal divided by that of the noise. The whole receiver excluding the output voltage buffer draws 2.27 mA in average from a 0.9V voltage supply, i.e. a power consumption of 2.04 mW.

## V. CONCLUSION

A fully integrated super-regenerative receiver in IBM 90-nm RF CMOS technology is designed to detect 500 MHz bandwidth UWB-FM signals at 4.5 GHz. Circuit simulations show that a receiver sensitivity of -83.3 dBm is attainable for

a 100 kbps baseband data-rate and  $10^{-6}$  potential bit-error-rate. The whole circuit draws an average of 2.3 mA from a 0.9 V supply. Comparing this work with other UWB-FM receivers, as shown in Table II, this super-regenerative receiver demonstrates higher sensitivity while consumes remarkably less power.

## REFERENCES

- [1] J. F. Gerrits and J. R. Farserotu., "Ultra wideband fm: A straightforward frequency domain approach," *European Microwave Conference, 2003. 33rd*, pp. 853–856, Oct. 2003.
- [2] J. Gerrits, J. Farserotu, and J. Long, "A wideband fm demodulator for a low-complexity fm-uwv receiver," *Wireless Technology, 2006. The 9th European Conference on*, pp. 99–102, Sept. 2006.
- [3] T. Tong, J. Mikkehen, and T. Larsen, "A 0.18  $\mu$ m cmos implementation of a low power, fully differential rf front-end for fm-uwv based p-pan receivers," *Communication systems, 2006. ICCS 2006. 10th IEEE Singapore International Conference on*, pp. 1–5, 30 2006–Nov. 1 2006.
- [4] E. H. Armstrong, "Signaling systems," *US Patent*, July 1922.
- [5] P. Favre, N. Joehl, A. Vouilloz, P. Deval, C. Dehollain, and M. Declercq, "A 2-v 600- $\mu$ Ea 1-ghz bicmos super-regenerative receiver for ism applications," *Solid-State Circuits, IEEE Journal of*, vol. 33, pp. 2186–2196, Dec 1998.
- [6] A. Vouilloz, M. Declercq, and C. Dehollain, "A low-power cmos super-regenerative receiver at 1 ghz," *Solid-State Circuits, IEEE Journal of*, vol. 36, pp. 440–451, Mar 2001.
- [7] N. Joehl, C. Dehollain, P. Favre, P. Deval, and M. Declercq, "A low-power 1-ghz super-regenerative transceiver with time-shared pll control," *Solid-State Circuits, IEEE Journal of*, vol. 36, pp. 1025–1031, Jul 2001.
- [8] J.-Y. Chen, M. Flynn, and J. Hayes, "A fully integrated auto-calibrated super-regenerative receiver in 0.13- $\mu$ Em cmos," *Solid-State Circuits, IEEE Journal of*, vol. 42, pp. 1976–1985, Sept. 2007.
- [9] I. McGregor, E. Wasige, and I. Thayne, "Sub-50 $\mu$ Ew, 2.4 ghz super-regenerative transceiver with ultra low duty cycle and a 675 $\mu$ Ew high impedance super-regenerative receiver," *Microwave Conference, 2007. European*, pp. 1322–1325, Oct. 2007.
- [10] B. Otis, Y. Chee, and J. Rabaey, "A 400  $\mu$ spl  $\mu$ w-rx, 1.6mw-tx super-regenerative transceiver for wireless sensor networks," *Solid-State Circuits Conference, 2005. Digest of Technical Papers. ISSCC. 2005 IEEE International*, pp. 396–606 Vol. 1, Feb. 2005.
- [11] F. Moncunill-Geniz, P. Pala-Schonwalder, C. Dehollain, N. Joehl, and M. Declercq, "An 11-mb/s 2.1-mw synchronous superregenerative receiver at 2.4 ghz," *Microwave Theory and Techniques, IEEE Transactions on*, vol. 55, pp. 1355–1362, June 2007.
- [12] F. Moncunill, O. Mas, and P. Pala, "A direct-sequence spread-spectrum super-regenerative receiver," *Circuits and Systems, 2000. Proceedings. ISCAS 2000 Geneva. The 2000 IEEE International Symposium on*, vol. 1, pp. 68–71 vol.1, 2000.
- [13] F. Moncunill-Geniz, P. Pala-Schonwalder, and F. del Aguila-Lopez, "New superregenerative architectures for direct-sequence spread-spectrum communications," *Circuits and Systems II: Express Briefs, IEEE Transactions on*, vol. 52, pp. 415–419, July 2005.
- [14] M. Pelissier, D. Morche, and P. Vincent, "Rf front end of uwv receiver based on super-regeneration," *Ultra-Wideband, 2007. ICUWB 2007. IEEE International Conference on*, pp. 180–183, Sept. 2007.
- [15] F. Xavier Moncunill-Geniz, P. Pala-Schonwalder, F. del Aguila-Lopez, and R. Giralt-Mas, "Application of the superregenerative principle to uwv pulse generation and reception," *Electronics, Circuits and Systems, 2007. ICECS 2007. 14th IEEE International Conference on*, pp. 935–938, Dec. 2007.
- [16] M. Anis, R. Tielert, and N. Wehn, "Fully integrated self-quenched super-regenerative uwv impulse detector," *Wireless Pervasive Computing, 2008. ISWPC 2008. 3rd International Symposium on*, pp. 773–775, May 2008.
- [17] H. Kalmus, "Some notes on superregeneration with particular emphasis on its possibilities for frequency modulation," *Proceedings of the IRE*, vol. 32, pp. 591–600, Oct. 1944.
- [18] L. Hernandez and S. Paton, "A superregenerative receiver for phase and frequency modulated carriers," *Circuits and Systems, 2002. ISCAS 2002. IEEE International Symposium on*, vol. 3, pp. III–81–III–84 vol.3, 2002.
- [19] J. Ayers, K. Mayaram, and T. Fiez, "A low power bfsk super-regenerative transceiver," *Circuits and Systems, 2007. ISCAS 2007. IEEE International Symposium on*, pp. 3099–3102, May 2007.